BPM31510 Increases the CoQ Pool in Chemically-Induced CoQ-Deficient Cells, CoQ-Deficient Patient Fibroblasts, and in Metabolically Active Murine Tissues

Juan J. Aristizabal-Henao[1], Sarah R. Wessel[1], Sylwia A. Stopka[1], Srada Karmacharya[1], Devon Van Cura[1], Alba Pesini[2], Kelsey R. Nickerson[1], Kashni Grover[1], Oksana Zavidij[1], Archna Ravi[1], Andressa L. Mota[1], Kenneth M. Rosen[1], Maria-Dorothea Nastke[1], Megan K. Cox[1], Brian Berman[1,3], Niven R. Narain[1,3], Vijay Modur[1], Catarina M. Quinzii[2], Stephane Gesta[1], Michael A. Kiebish[1]

[1]BPGbio Inc., Waltham, MA, USA; [2] Columbia University, New York, NY, USA; [3] Department of Molecular Biology and Department of Dermatology and Cutaneous Surgery, University of Miami Miller School of Medicine, Miami, FL

ABSTRACT

Coenzyme Q10 (CoQ10) is an essential lipid-soluble redox cofactor that supports mitochondrial electron transport and ATP production. Despite its clinical use, oral CoQ10 supplementation is hindered by poor oral bioavailability and limited tissue uptake. BPM31510 is a novel injectable formulation of oxidized CoQ10, designed to enhance systemic exposure and mitochondrial delivery. This study evaluated the capacity of BPM31510 to enhance CoQ levels to restore cellular function across distinct models of CoQ deficiency.

In vitro studies employed SH-SY5Y neuroblastoma cells with chemically induced CoQ10 deficiency via para-aminobenzoic acid (PABA) administration. Quantification of oxidized CoQ10, reduced CoQ10, and oxidized CoQ9 were performed using Ultra-High Performance Liquid Chromatography-Tandem Mass Spectrometry (UHPLC-MS/MS). Treatment with BPM31510 resulted in significant increases in all three analyzed CoQ species compared to solubilized CoQ10. Furthermore, BPM31510 treatment demonstrated efficacy in restoring ATP content, necessary for improved mitochondrial energy production. BPM31510's ability to restore CoQ10 levels was further demonstrated in patient-derived fibroblasts carrying pathogenic mutations in either PDSS2, COQ2 or COQ8A genes, outperforming solubilized CoQ10 in these genetic CoQ10 deficiency models.

To determine if BPM31510 overcomes the limitations of oral bioavailability, its systemic exposure and tissue uptake were evaluated in C57BL/6J mice. To that end, animals received either BPM31510 (10 or 50 mg/kg, intraperitoneal) or oral CoQ10 twice daily for 14 days. Analysis of plasma and tissues by UHPLC-MS/MS revealed that BPM31510 administration substantially increased the overall tissue CoQ pool relative to oral CoQ10. Spatial distribution of CoQ10 was investigated using Matrix-Assisted Laser Desorption/Ionization (MALDI) mass spectrometry imaging, which confirmed accumulation of oxidized CoQ10 in a mouse model of CoQ10 deficiency (*Coq4^{F147C}* mice) which revealed increased tissue spatial distribution in brain (cerebellum) and kidney. Taken together, these results highlight efficient CoQ10 delivery to metabolically active tissues.

In summary, these data demonstrate that BPM31510 restores CoQ levels in chemically induced and genetic models of CoQ deficiency and enhances delivery of bioactive CoQ10 into metabolically active tissues *in vivo*. Further investigation is warranted to determine whether BPM31510, by effectively overcoming absorption and distribution limitations associated with conventional oral CoQ10 supplementation, may provide benefit in primary or secondary CoQ10 deficiencies, as well as in broader mitochondrial and metabolic disorders characterized by impaired redox balance and disrupted energy homeostasis.

Figure 1: BPM31510 and Primary CoQ10 Deficiency

Challenges in Development of CoQ10 as a Therapy

- Poor oral bioavailability (<0.1%)
- Lack of pharmaceutical cGMP grade product/formulations for IV, subQ, topical, or oral formulations
- Low PK/PD ratios to effectuate mitochondrial function at tissue level
- A true lack of the translational potential of the molecule in mainstream medicine and pharmaceutical ecosystem

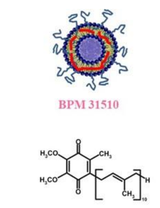

- Proprietary & stable formulation
- Contains CoQ10 and nanoparticle lipid membrane to modify mitochondrial metabolism
- A bio-membrane -like capsule
- Enrichment in mitochondria
- Well-tolerated with a favorable safety profile

Primary CoQ10 Deficiency (PCQD)

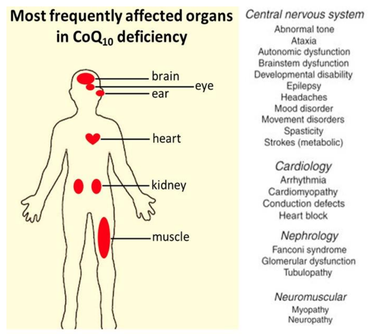

Wang et al J Cell Mol Med Sept 2022 26(17):4635-4644

Figure 2: Chemically Induced CoQ10 Deficiency In Vitro

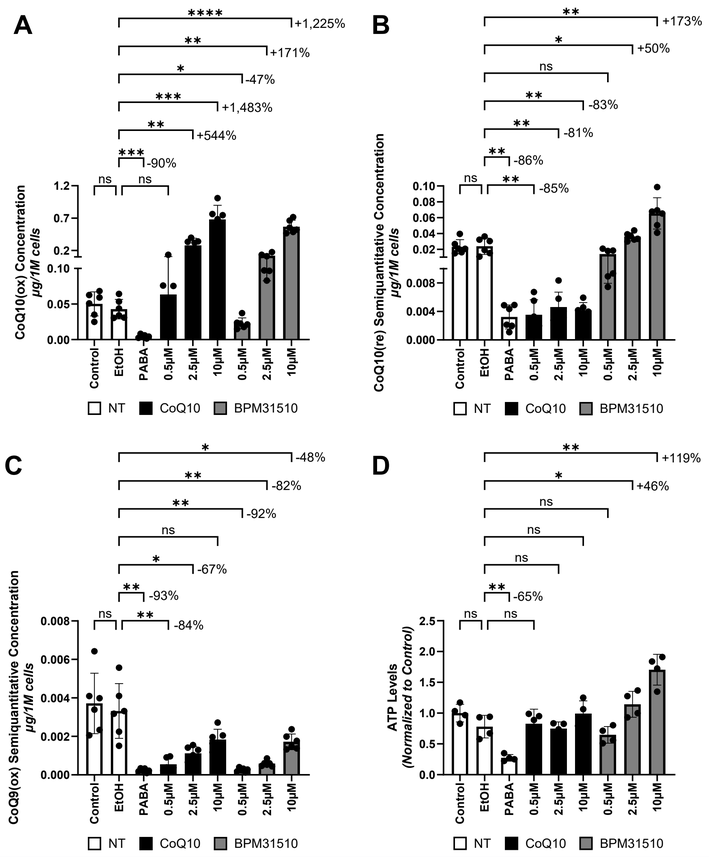

Figure 2: SH-SY5Y cells: Non-treated (NT; Control and Ethanol vehicle), treated with para-aminobenzoic acid (PABA) to induce depletion of the CoQ pool, and treated with PABA and increasing doses of CoQ10 or BPM31510. **(A)** Absolute CoQ10(ox) concentrations; **(B)** Semiquantitative CoQ10(re) concentrations; **(C)** Semiquantitative CoQ9(ox) concentrations; **(D)** relative ATP levels. Data are presented as concentrations in µg per 1 million cells, mean ± standard deviation. Statistical significance was inferred at: *p < 0.05, **p < 0.01, ***p < 0.001, ****p < 0.0001; ns, not significant.

Figure 3: BPM31510 Increases Content and Bioactivity Of CoQ10 In Primary CoQ10 Deficiency Patient Fibroblasts Compared To CoQ10 Treatment Alone

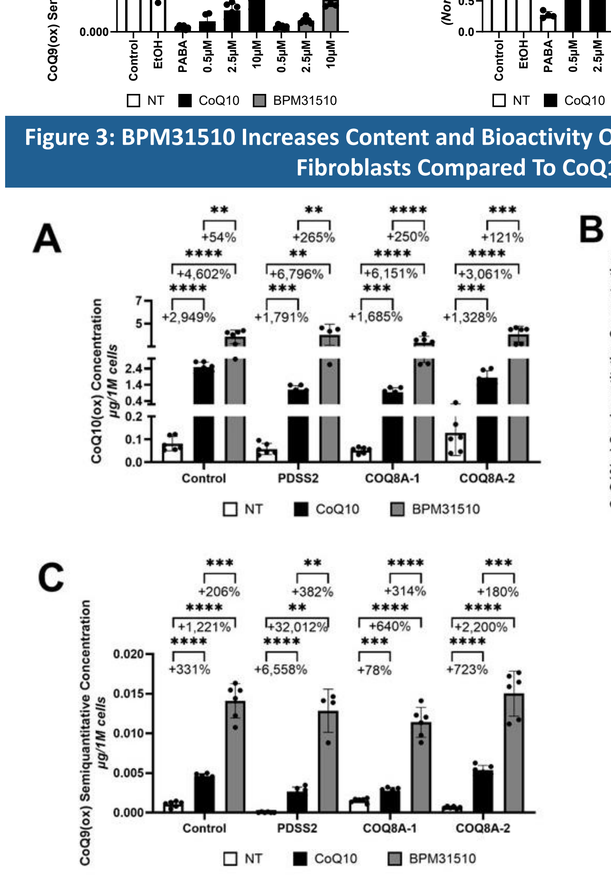

Figure 3: Control, PDSS2, COQ8A-1 and COQ8A-2 fibroblasts: Non-treated (NT), treated with 5 µM solubilized CoQ10 or 5 µM BPM31510. **(A)** Absolute CoQ10(ox) concentrations; **(B)** Semiquantitative CoQ10(re) concentrations; **(C)** Semiquantitative CoQ9(ox) concentrations. Data are presented as concentrations in µg per 1 million cells, mean ± standard deviation. Statistical significance was inferred at: *p < 0.05, **p < 0.01, ***p < 0.001, ****p < 0.0001; ns, not significant. PDSS2: patient 2, COQ8A-1: patient 2 and CoQ8A-2: patient 3.

Figure 4: LC MS/MS And Spatial Quinomics And Metabolomics Analyses

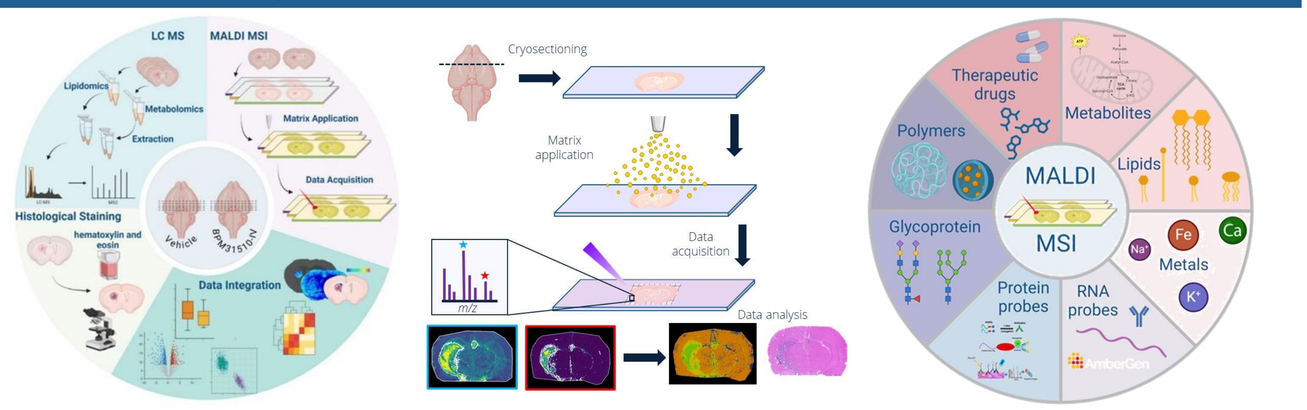

Figure 4: LC MS/MS and spatial metabolomics and quinomics were utilized to quantitatively assess CoQ levels and quinone metabolites in various rodent tissues.

Figure 5: Plasma And Tissue CoQ Levels Between Oral (PO) CoQ10 Versus Intraperitoneal (IP) BPM31510 Dosing

Wild type 2 week PO and IP Dosing Study

- 10 mg/kg BID (MBS CoQ10 Oral Formulation)
- 10 mg/kg BID IP BPM31510
- 50 mg/kg BID (MBS CoQ10 Oral Formulation)
- 50 mg/kg BID IP BPM31510

Goal: Evaluate Tissue Distribution of CoQ10 comparing conventional oral formulation relative to IP BPM31510 in a dose dependent manner

Samples: Plasma, Cerebellum, kidney, gastrocnemius muscle, heart, liver, adipose tissues

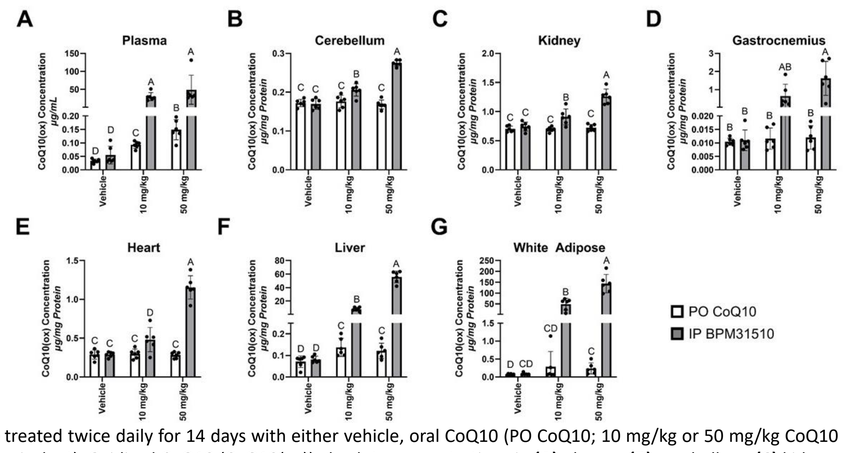

Figure 5: Oxidized CoQ10 levels in tissues from C57BL/6J mice treated twice daily for 14 days with either vehicle, oral CoQ10 (PO CoQ10; 10 mg/kg or 50 mg/kg CoQ10 equivalent), or BPM31510 (IP; 10 mg/kg or 50 mg/kg CoQ10 equivalent). Oxidized CoQ10 (CoQ10(ox)) absolute concentrations in **(A)** plasma, **(B)** cerebellum, **(C)** kidney, **(D)** gastrocnemius, **(E)** heart, **(F)** liver, and **(G)** white adipose tissue. Bars labeled with different letters (e.g., A, B, C, D) are significantly different from each other ($p < 0.05$) within each tissue type, as determined by one-way ANOVA. Bars that share a letter are not statistically different. PO, oral; IP, intraperitoneal.

Figure 6: Experimental Design And Multimodal Analysis Pipeline To Assess Delivery Of BPM31510 To Increase CoQ_{10} Levels In Coq4$^{+/+}$ Or *Coq4^{F147C}* Mice

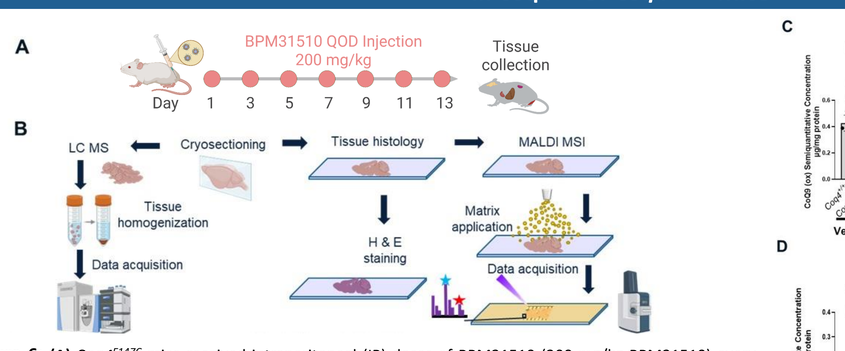

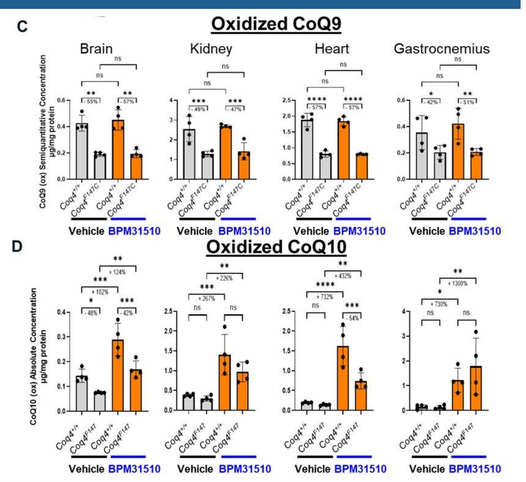

Figure 6: (A) *Coq4^{F147C}* mice received intraperitoneal (IP) doses of BPM31510 (200 mg/kg BPM31510) every other day for a total of 2-weeks and **(B)** corresponding tissue processing **(C)** LC-MS/MS analysis of oxidized CoQ_9 in brain, kidney, heart, and gastrocnemius from *Coq4$^{+/+}$* and *Coq4^{F147C}* mice treated with vehicle or BPM31510. **(D)** LC-MS/MS quantification of oxidized CoQ_{10} in brain, kidney, heart, and gastrocnemius from Coq4$^{+/+}$and Coq4^{F147C} mice treated with vehicle or BPM31510. Data are represented as ug per mg of protein (mean±SD, n≥4 per group). *p < 0.05, **p < 0.01, ***p < 0.001; ns = not significant (One-way Anova), ox = oxidized

Figure 7: BPM31510 Treatment Increases CoQ_{10} Levels In Cerebellum Of CoQ10 Deficiency Mouse Model

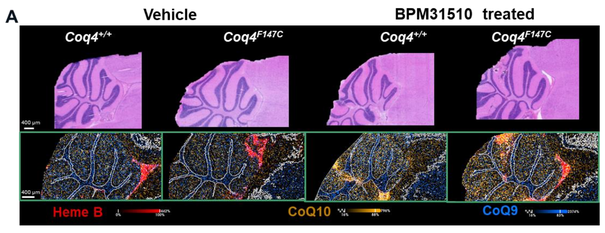

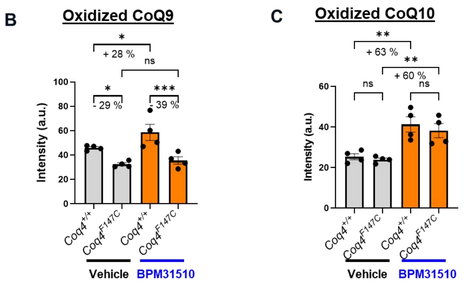

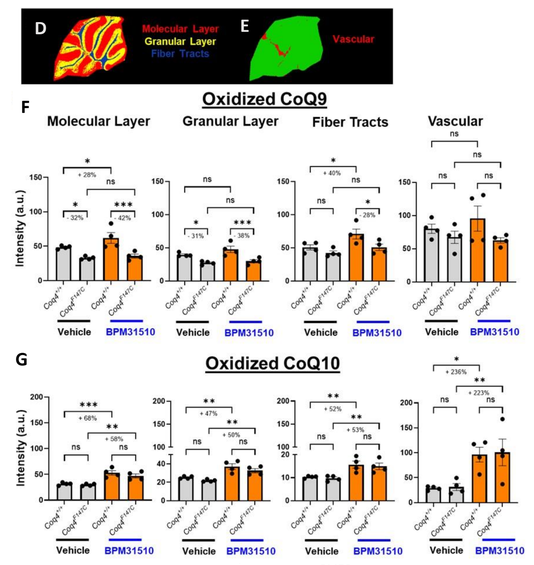

Figure 7: (A) Representative H&E sections and MALDI-MSI composite ion images of sagittal cerebellum sections from *Coq4$^{+/+}$*and *Coq4^{F147C}* mice treated with vehicle or BPM31510. Ion distributions of heme B (red), CoQ_{10} (yellow), and CoQ_9 (blue) are shown. Average ion signal of **(B)** CoQ_9 and **(C)** CoQ_{10} in the whole cerebellar region from *Coq4$^{+/+}$*and *Coq4^{F147C}* mice treated with vehicle or BPM31510. Data are represented as intensity a.u.) (mean±SD, n≥4 per group). *p < 0.05, **p < 0.01, ***p < 0.001; ns = not significant (One-way Anova). Segmentation map defining the molecular layer, granular layer, the fiber tracts **(D)**, and vascular **(E)** regions that were utilized for quantifying spatial distribution. Semi-quantitative MALDI-MSI intensity analysis of **(F)** CoQ_9 and **(G)** CoQ_{10} in the defined cerebellar regions. Data are represented as intensity (a.u.) (mean±SD, n≥4 per group). *p < 0.05, **p < 0.01, ***p < 0.001; ns = not significant (One-way Anova).

Figure 8: BPM31510 Increases CoQ10 Levels In Different Kidney Regions Of A Mouse Model of CoQ10 Deficiency

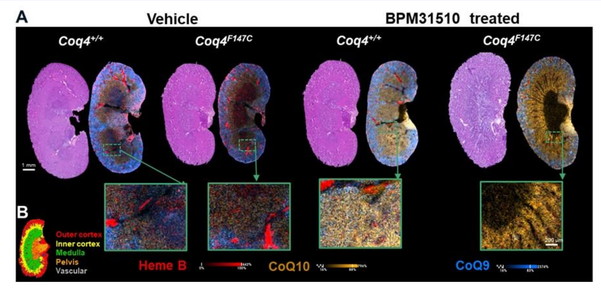

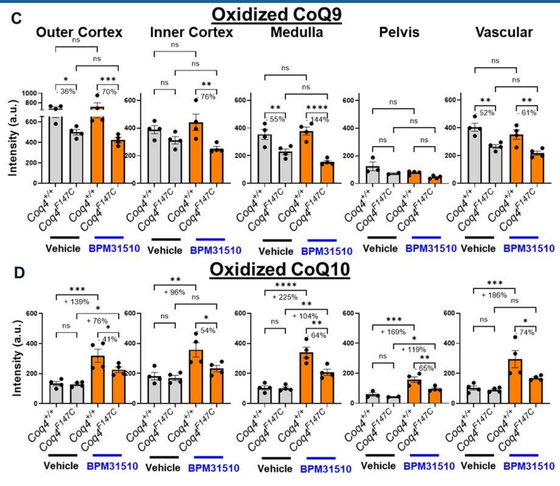

Figure 8: Spatial distribution and semi-quantitative analysis of CoQ species within the kidney (A) Representative H&E sections and MALDI-MSI composite ion images of sagittal kidney sections from *Coq4$^{+/+}$*and *Coq4^{F147C}* mice treated with vehicle or BPM31510. Ion distributions of heme B (red), CoQ_{10} (yellow), and CoQ_9 (blue) are shown. **(B)** Segmentation map defining the outer cortex (red), inner cortex (yellow), medulla (green), pelvis (orange), and vascular (white) subregions for quantifying spatial distribution. Semi-quantitative MALDI-MSI intensity analysis of **(C)** CoQ_9 and **(D)** CoQ_{10} in the defined kidney regions. Data are represented as intensity (a.u.) (mean±SD, n≥4 per group). *p < 0.05, **p < 0.01, ***p < 0.001; ns = not significant (One-way Anova).

Conclusions

- **BPM31510 demonstrated increased delivery of CoQ10 and bioactivity in a chemically induced model of CoQ10 Deficiency as well as in patient-derived fibroblasts.**
- **BPM31510 IP injection also demonstrated enhanced tissue distribution compared to oral CoQ10 in tissues (e.g., brain, kidney, muscle) which inherently exhibit bioenergetic deficiencies in mitochondrial diseases (*Wang et al., 2022*).**
- **Spatial quinomics analysis demonstrated that BPM31510 was able to deliver CoQ10 to the cerebellum (a key region governing ataxia in PCQD) as well as delivering CoQ10 to subregions within the cerebellum in a mouse model of CoQ10 deficiency**
- **Spatial analysis of kidney (another tissue impacted in PCQD) also demonstrated that BPM31510 was able to deliver CoQ10 to different functional regions of the kidney.**
- **BPM31510 has demonstrated its potential ability to overcome several of the challenges with treating PCQD demonstrating its bioactivity and tissue delivery, which are critical components for the development of CoQ10 as an effective therapy.**